Supporting Information for

Fluoroalkyl-Modified Naphthodithiophene Diimides

Wei Fan, Chunming Liu, Yan Li, and Zhaohui Wang

Table of contents

1. Materials and Methods:

^{1}H NMR and ^{13}C NMR spectra were recorded in deuterated solvents on a Bruker AVANCE 400 NMR Spectrometer and a Bruker AVIII 500WB NMR Spectrometer. ^{1}H NMR chemical shifts are reported in ppm downfield from tetramethylsilane (TMS) reference using the residual protonated solvent as an internal standard. Mass spectra (MALDI-TOF-MS) were determined on a Bruker BIFLEX III Mass Spectrometer. Absorption spectra were measured with Hitachi (model U-3010) UV-Vis spectrophotometer in a 1-cm quartz cell. Cyclic voltammetry (CV) was performed with a Zahner IM6e electrochemical workstation using glassy carbon discs as the working electrode, Pt wire as the counter electrode, Ag/AgCl electrode as the reference electrode. 0.1 M tetrabutylammonium hexafluorophosphate ($TBAPF_6$) dissolved in CH_2Cl_2 was employed as the supporting electrolyte. The plot includes the signal of the ferrocene as an internal potential marker. CH_2Cl_2 was freshly distilled prior to use.

All chemicals were purchased from commercial suppliers and used without further purification unless otherwise specified.

2. Synthesis and characterization of compounds

The starting material (triisopropylsilyl)acetylene was purchased from commercial suppliers and used without further purification unless otherwise specified. Compounds **1** and **5** were synthesized according to literature procedures. [1, 2]

Compound [(triisopropylsilyl)ethynyl]copper(I):

(Triisopropylsilyl)acetylene (100 mg, 0.548 mmol) was dissolved in dry DMF (30 ml) , CuI (103 mg, 0.548 mmol) was added into the solution and stirred at room temperature for 30 mins under nitrogen atmosphere. Then Et_3N (0.16 mL, 1.1 mmol) was added, the solution was stirred for another 30mins. The reaction mixture was poured in water and collect the solid by suction filtration to afford compound [(triisopropylsilyl)ethynyl]copper(I) (131 mg, 98%) as a yellow solid.

Compound 2:

The solution compound [(triisopropylsilyl)ethynyl]copper(I) (0.82 g, 3.36 mmol) and **1** (1.0 g, 1.34 mmol) in dry DMSO (30 mL) was stirred at 100°C for 0.5 h. The reaction mixture was poured in water and collect the solid by suction filtration. The residue was purified by silica gel chromatography (dichloromethane: petroether = 1:1) to afford compound **2** (1.2 g, 95%) as a yellow solid.

^{1}H NMR (400 MHz, 298 K, $CDCl_3$, ppm) δ = 8.88 (s, 2H), 7.52-7.48 (t, *J* = 8Hz, 2H), 7.34-7.32 (d, *J* = 8Hz, 4H), 2.76-2.65 (m, 4H), 1.18-1.14 (m, 66H). ^{13}C NMR (100 MHz, $CDCl_3$, ppm) δ = 162.1, 160.7, 145.7, 138.2, 130.3, 129.6, 127.6, 127.2, 125.4, 124.0, 108.8, 104.8, 29.3, 24.0, 23.8, 18.6, 11.3. HRMS (MALDI, 100%) m/z calcd (%) for $C_{60}H_{78}N_2O_4Si_2$: 945.5506, found 945.5507

Compound 3:

The solution compound **2** (200 mg, 0.22 mmol) and $Na_2S{\cdot}9H_2O$ (317 mg, 1.32 mmol) in ethonal (200 ml) and Acetic acid (4 ml) was stirred at 60°C for 20 h under nitrogen atmosphere. The reaction mixture was poured in water and the product was extracted with CH_2Cl_2. The combined organic layers were washed with water and dried over $MgSO_4$ to afford intermediate. The intermediate was dissolved in THF, TBAF (4 mL) was added. The mixture solution was stirred at

60°C for 5 h. The reaction mixture was poured in water and collect the solid by suction filtration, the residue was purified by silica gel chromatography (dichloromethane: petroether = 1:3) to afford compound **3** (53 mg, 35%) as a red solid.

^{1}H NMR (400 MHz, 298 K, $CDCl_3$, ppm) δ = 9.05-9.03 (d, *J* = 8Hz, 2H), 8.21-8.20 (d, *J* = 4Hz, 2H), 7.59-7.55 (t, *J* = 8Hz, 2H), 7.43-7.41 (d, *J* = 8Hz, 4H), 2.83-2.77 (m, 4H), 1.21-1.18 (m, 24H). ^{13}C NMR (100 MHz, $CDCl_3$, ppm) δ = 163.5, 163.4, 145.8, 145.6, 143.6, 141.2, 130.3, 130.1, 124.5, 123.6, 119.2, 118.1, 29.4, 24.0. HRMS (MALDI, 100%) m/z calcd (%) for $C_{42}H_{38}N_2O_4S_2$: 698.2278, found 698.2278

Compound 4:

The solution compound **3** (100 mg, 0.143 mmol), nanometer copper powder (10eq) and 1,1,1,2,2,3,3,4,4-nonafluoro-4-iodobutane (495 mg, 1.43 mmol) in dry DMSO (4 mL) was stirred at 120°C for 12 h under nitrogen atmosphere. The reaction mixture was poured in water and the product was extracted with CH_2Cl_2. The combined organic layers were washed with water and dried over $MgSO_4$. After removal of the solvent under vacuum, the residue was purified by silica gel chromatography (dichloromethane: petroether = 1:5) to afford compound **4** (32.5mg, 20%) as a red solid.

^{1}H NMR (400 MHz, 298 K, $CDCl_3$, ppm) δ = 9.43 (s, 2H), 7.61-7.57 (t, *J* = 8Hz, 2H), 7.44-7.42 (d, *J* = 8Hz, 4H), 2.78-2.71 (m, 4H), 1.21-1.18 (m, 24H). ^{13}C NMR (100 MHz, $CDCl_3$, ppm) δ = 163.0, 162.7, 145.6, 145.5, 142.1, 130.4, 129.4, 127.8, 124.5, 119.9, 119.7, 29.5, 24.1, 23.9. HRMS (MALDI, 100%) m/z calcd (%) for $C_{50}H_{36}F_{18}N_2O_4S_2$: 1134.1835, found 1134.1840

Compound 6 was synthesized according to the compound **2** procedure.

^{1}H NMR (400 MHz, 298 K, $CDCl_3$, ppm) δ = 8.85 (s, 2H), 5.16-4.48 (m, 4H), 1.56-1.20 (m, 42H). ^{13}C NMR (100 MHz, $CDCl_3$, ppm) δ = 161.6, 160.2, 138.4, 128.0, 126.5, 125.9, 124.7, 110.4, 104.3, 38.6, 18.6, 11.3. HRMS (MALDI, 100%) m/z calcd (%) for $C_{44}H_{48}F_{14}N_2O_4Si_2$: 990.2935, found 990.2934

Compound 7

The solution compound **6** (200 mg, 0.20 mmol) and $Na_2S{\cdot}9H_2O$ (291 mg, 1.21 mmol) in ethonal (200 ml) and acetic acid (4 ml) was stirred at 60°C for 20 h under nitrogen atmosphere. The reaction mixture was poured in water and the product was extracted with CH_2Cl_2. The combined organic layers were washed with water and dried over $MgSO_4$. Then the mixture was purified by silica gel chromatography (dichloromethane: petroether = 1:4) to afford compound **7** (63mg, 30%) as a red solid.

^{1}H NMR (400 MHz, 298 K, $CDCl_3$, ppm) δ = 9.19 (s, 2H), 5.25-5.17 (t, *J*=16Hz, 4H), 1.25-1.23 (d, *J*=8Hz, 42H). ^{13}C NMR (100 MHz, $CDCl_3$, ppm) δ = 163.0, 162.7, 156.4, 149.0, 144.2, 132.0, 122.9, 117.9, 116.7, 29.7, 18.7, 11.9. HRMS (MALDI, 100%) m/z calcd (%) for $C_{44}H_{48}F_{14}N_2O_4S_2Si_2$: 1054.2376, found 1054.2374

Compound 8

The compound **7** (100 mg, 0.09 mmol) was dissolved in THF, TBAF (2 mL) was added. The mixture solution was stirred at 60°C for 5 h. The reaction mixture was poured in water and collect the solid by suction filtration to afford compound **8** (70 mg, 100%) as a red solid.

^{1}H NMR (500 MHz, 373 K, $CDCl_2CDCl_2$, ppm) δ = 9.05-9.04 (d, *J* = 5Hz, 2H), 8.27-8.26 (d, *J*= 5 Hz, 2H), 5.24-5.18 (t, *J* = 15Hz, 4H). ^{13}C NMR was not taken due to its low signal. HRMS (MALDI, 100%) m/z calcd (%) for $C_{26}H_8F_{14}N_2O_4S_2$: 741.9707, found 741.9707.

3. Computational methods

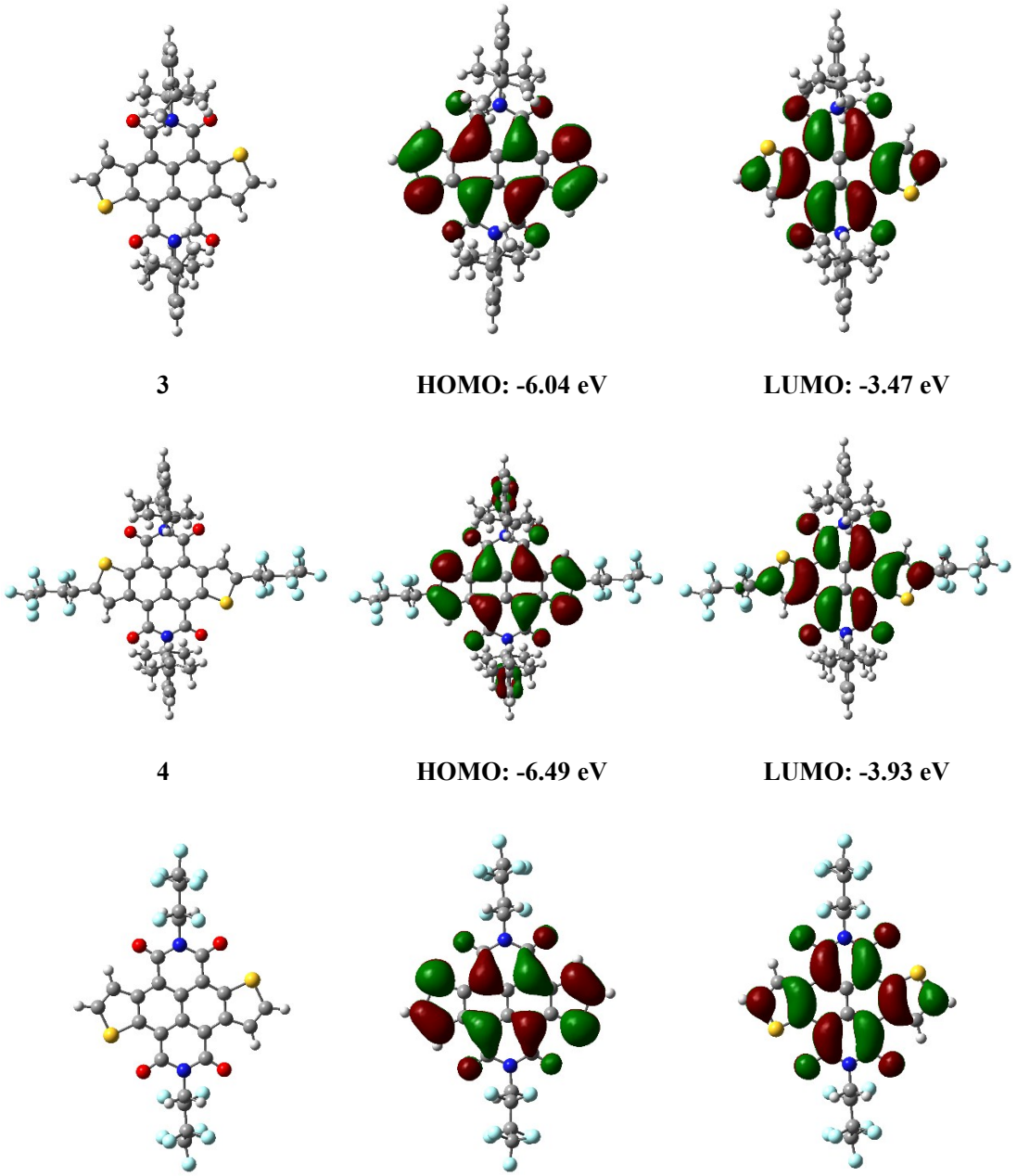

Figure S1. Molecular geometry and frontier molecular orbitals of three NDTI derivatives calculated at the DFT-B3LYP/6-31G(d,p) level.

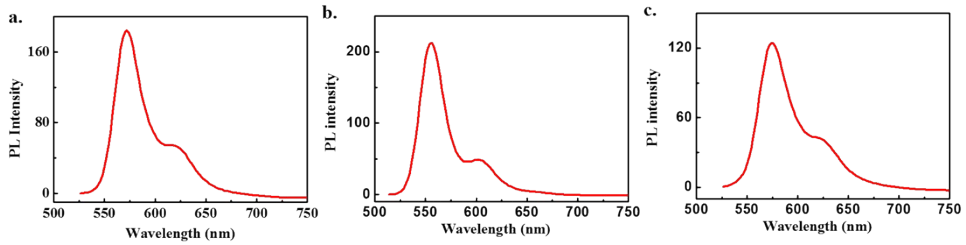

Figure S2. The emission spetra of compounds: (a) compound 3, λ_{ex} = 516 nm, Φ_{fl} = 2.0 %; (b) compound 4, λ_{ex} = 504 nm, Φ_{fl} = 1.1 %; (c) compound 4, λ_{ex} = 516 nm, Φ_{fl} = 3.3 %. The emission quantum yield of **3**, **4** and **8** in $CHCl_3$ were determined using Rhodamine B in water (Φ_{fl} = 31 %; excited at 514 nm) as the standard.

4. X-ray crystallographic analysis

Crystallographic data have been deposited with the Cambridge Crystallographic Data Centre as supplementary publication no. CCDC 1494663 (**3**), 1494664 (**4**), 1494665 (**8**). The measurements were made on a Bruker SMART CCD area detector with graphite monochromated Mo-Kα radiation (λ = 1.54178 Å) at 173(2) K. All calculations were performed using the SHELXL-973 and the CrystalStructure crystallographic software package. The crystallographic data were summarized in **Table S1**.

Table S1. Crystallographic data of three molecules.

Compound Reference	**3**	**4**	**8**
Crystal system	triclinic	triclinic	monoclinic
Space group	P$\bar{1}$	P$\bar{1}$	$P2_1/c$
Calculated density	1.277	1.537	1.912
Longitudinal shift (Å)	4.81	0.01	/
Transverse shift (Å)	2.66	5.57	/
Torsion angle (deg)	/	/	77.87 (torsion)
Interplanar distance (Å)	6.96	3.63	3.40
Packing mode	Slipping 1D Staking	Slipping 1D Staking	Torsion cofacial staking
Chemical formula	$C_{42.77}H_{39.54}Cl_{1.54}N_2O_4S_2$	$C_{50}H_{36}F_{18}N_2O_4S_2$	$C_{26}H_8F_{14}N_2O_4S_2$
Formula weight	764.25	1134.93	742.46
a (Å)	8.9017(18)	6.6539(13)	28.23(2)
b (Å)	9.2639(19)	13.569(3)	11.002(9)
c (Å)	13.141(3)	14.640(3)	8.319(7)
α (°)	97.10(3)	71.22(3)	90
β(°)	101.59(3)	78.76(3)	93.130(11)

γ (°)	107.30(3)	84.06(3)	90
Unit cell volume ($Å^3$)	993.8(4)	1226.2(5)	2580(4)
Temperature (K)	173.15	173.15	173.15
No. of formula units per unit cell	1	1	4
No. of reflections measured	11646	11922	4616
No. of independent reflections	4518	5584	4616
Rint	0.0431	0.0646	0.0752
Final R1 [I>2sigma(I)]	0.0774	0.0913	0.1312

5. Device fabrication and characterization

Device fabrication. The substrates used here were successively cleaned with pure water, piranha solution (H_2SO_4/H_2O_2=2:1), pure water, isopropyl alcohol, and finally were blown dry with high-purity nitrogen gas. Treatment of the Si/SiO_2 wafers with octadecyltrichlorosilane (OTS) was carried out with the vapor-deposition method. The traditional top-contact bottom-gate devices based on the nano/micro-single crystal were fabricated respectively with the organic nanowire mask method. Firstly, an individual micrometre or sub-micrometre organic nanowire made in advance was put directly on a crystal perpendicularly to the growth direction. Secondly, a layer of Au about 50 nm thick was deposited as the source and drain electrodes. Finally, the organic nanowires were removed and a transistor with two electrodes was obtained. All electrical characteristics of the devices were measured at room temperature using a semiconductor parameter analyser (Keithley 4200 SCS).

Micro/nanometer-sized single-crystals: Micro/nanometer-sized single-crystals of these compounds used in this study were prepared by solution drop-casting. The microscopic images of all the microcrystal were acquired by an optical microscopy (Vision Engineering Co., UK) (**Figure S3**), which was coupled to a CCD camera. Transmission electron microscopy (TEM) (**Figure S4**) and selected area electron diffraction (SAED) measurements were carried out using a TECNAI T20 electron microscope (FEI, USA) (**Figure S5**). X-ray diffraction (XRD) was measured on a D/max2500 with a CuKα source (κ = 1.541 Å) (**Figure S6**).

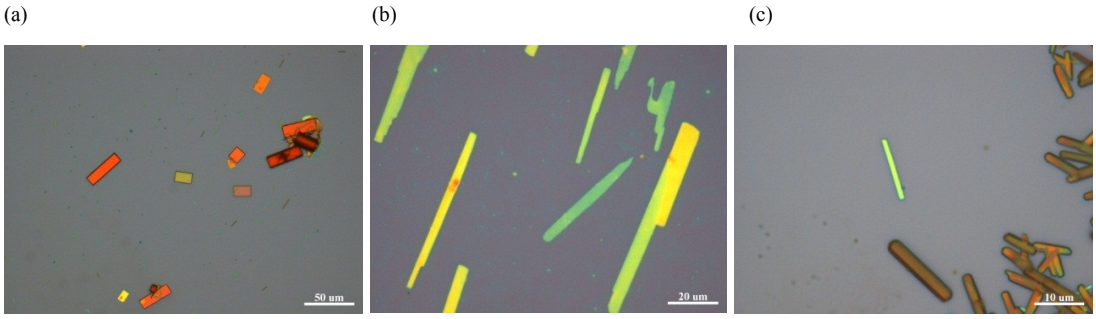

Figure S3. The optical microscopy (OM) image of single crystal microribbon of (a) compound **3**, (b) compound **4**, (c) compound **8**.

(a) (b) (c)

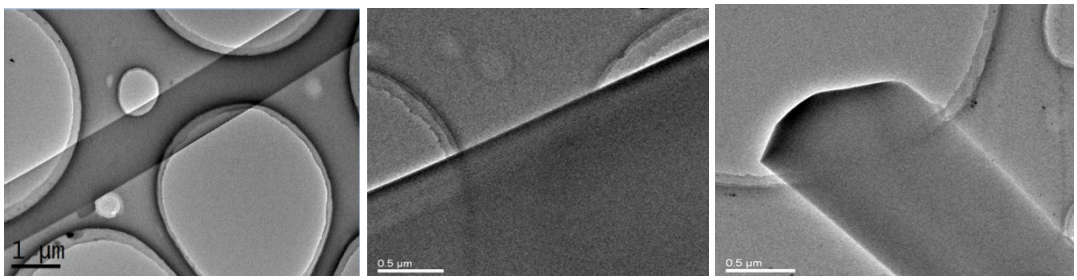

Figure S4. The transmission electron microscopy (TEM) images of single crystal microribbon of (a) compound **3**, (b) compound **4**, (c) compound **8**.

(a) (b) (c)

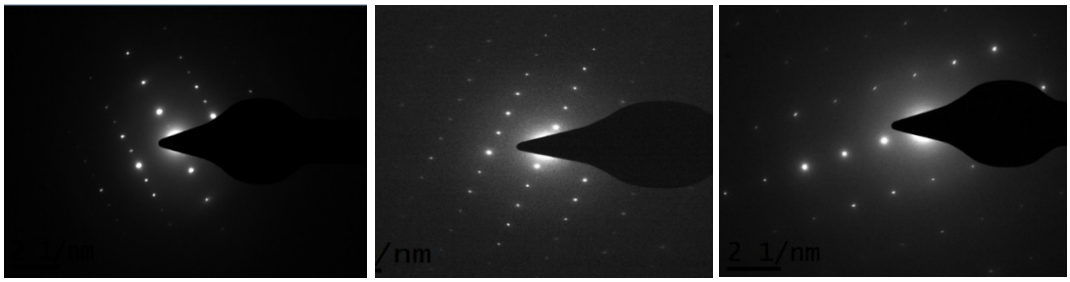

Figure S5. The SEAD patterns of single crystal microribbon of (a) compound **3**, (b) compound **4**, (c) compound **8**.

Micrometer-sized single crystals were prepared by solution drop-casting. We can learn from the single-crystal X-ray data, powder X-ray diffraction (XRD) pattern and the SAED pattern of compound **3** micro/nanometer-sized single-crystals that the b-axis was standing on the substrate, while the a–c plane was arranged parallel to the substrate. The powder X-ray diffraction (XRD) pattern and the SAED pattern of compound **4** micro/nanometer-sized single-crystals reveal that the c-axis was standing on the substrate, while the a–b plane was arranged parallel to the substrate. The powder X-ray diffraction (XRD) pattern and the SAED pattern of compound **8** micro/nanometer-sized single-crystals reveal that for compound **8** the a-axis was standing on the substrate, while the b–c plane was arranged parallel to the substrate.

(a) (b) (c)

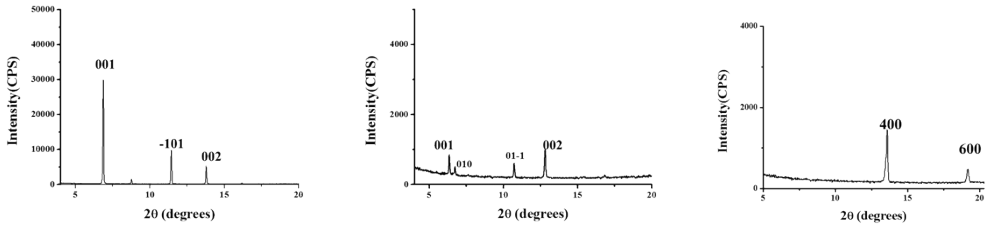

Figure S6. The powder X-ray diffraction (XRD) pattern of (a) compound **3**, (b) compound **4**, (c) compound **8**.

The traditional top-contact bottom-gate field-effect transistors based on the micrometer-sized single crystals were all measured under ambient conditions. Because of the loose arrangement and the absence of π-π stacking, effective charge-transporting channels could not be formed in

compound **3** single-crystals. OFET devices based on compound **3** single crystals exhibited neither n-type nor p-type performance. OFET devices based on compound **4** single crystals exhibited n-type semiconducting behaviors with an average electron mobility of 0.037 $cm^2 V^{-1} s^{-1}$ and the highest electron mobility of 0.065 $cm^2 V^{-1} s^{-1}$. compound **8**-based single-crystal OFETs exhibited relatively better n-type performance with an average electron mobility of 1.27 $cm^2 V^{-1} s^{-1}$ and the highest electron mobility of 1.59 $cm^2 V^{-1} s^{-1}$ for ribbon crystals based on about 30 devices. The single crystals of NDTIs 4 and 8 possess good device stability under ambient conditions (keeping the same order of magnitude within two weeks).

6. References:

(1) S. Chopin, F. Chaignon, E. Blart and F. Odobel, *J. Mater. Chem.* **2007**, *17*, 4139-4146.
(2) Z. Yuan, Y. Ma, T. Geβner, M. Li, L. Chen, M. Eustachi, R. T. Weitz, C. Li and K. Müllen, *Org. Lett.* **2016**, *18,* 456–459

7. ^{1}H and ^{13}C NMR Spectra

^{1}H NMR spectrum of **2** in $CDCl_3$

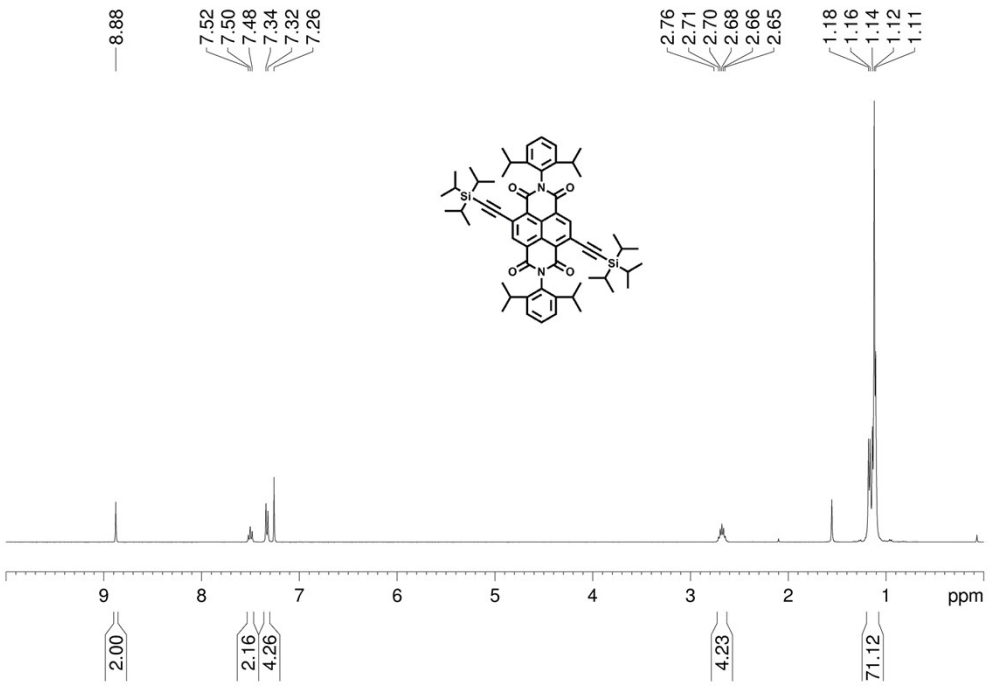

^{13}C NMR spectrum of **2** in $CDCl_3$

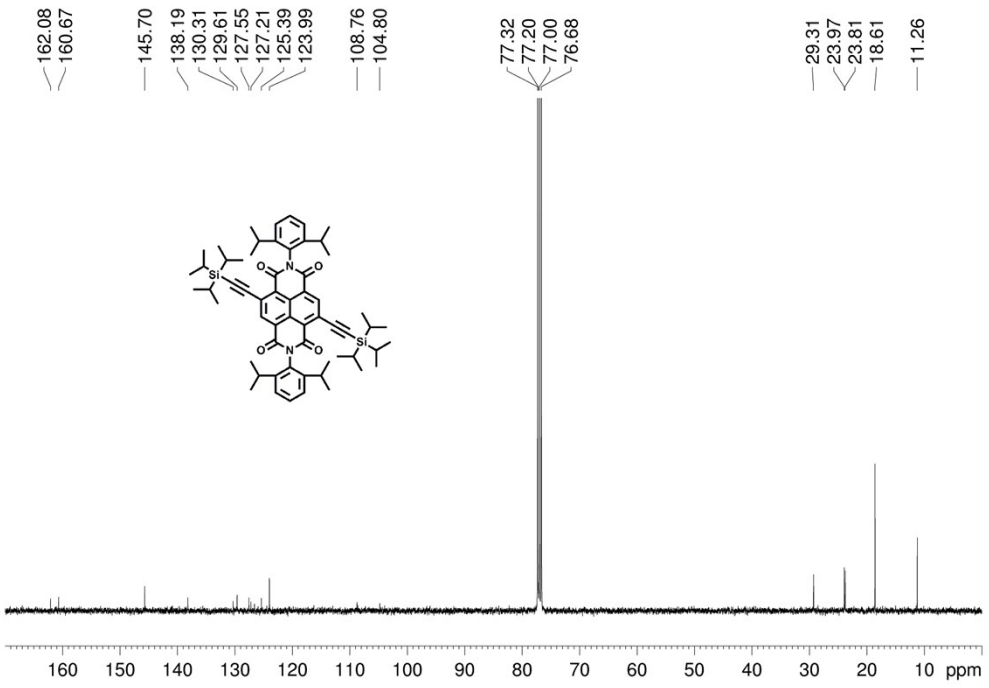

^{1}H NMR spectrum of **3** in $CDCl_3$

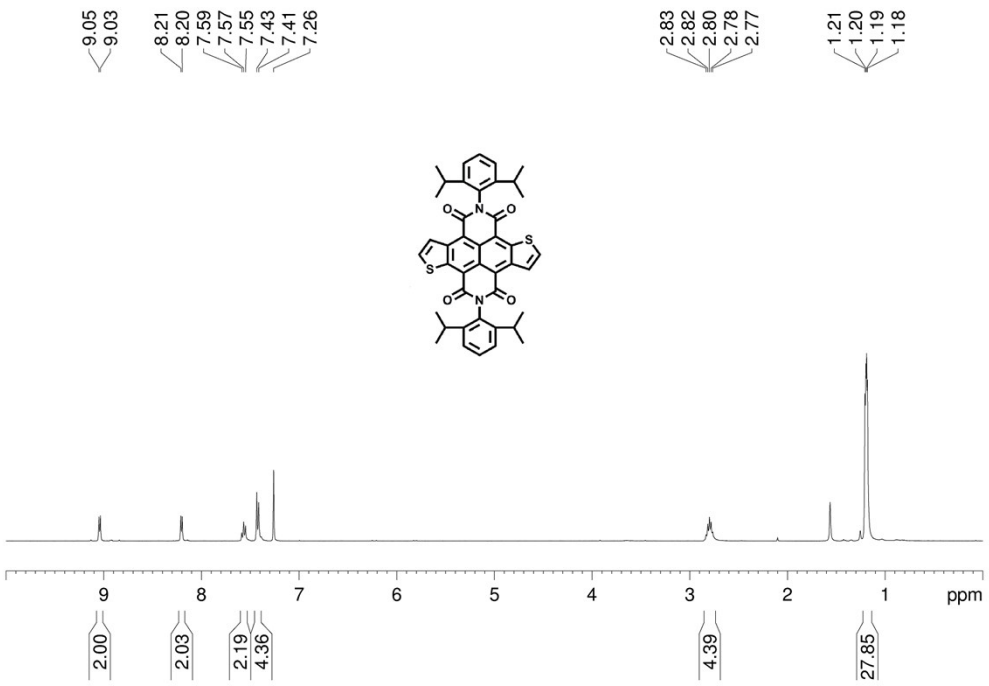

^{13}C NMR spectrum of **3** in $CDCl_3$

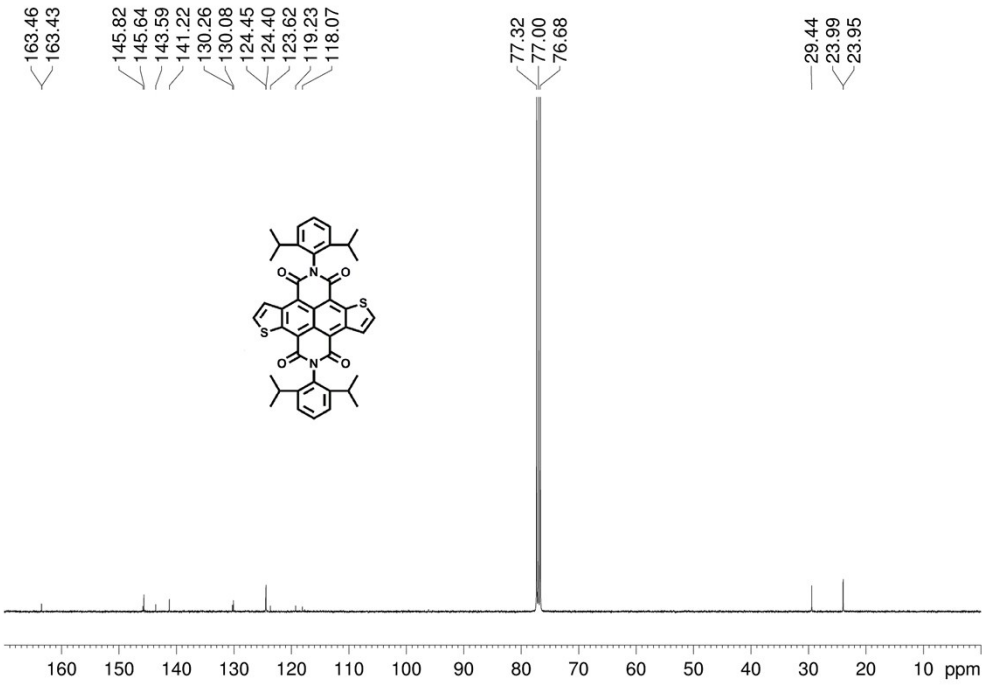

^{1}H NMR spectrum of **4** in $CDCl_3$

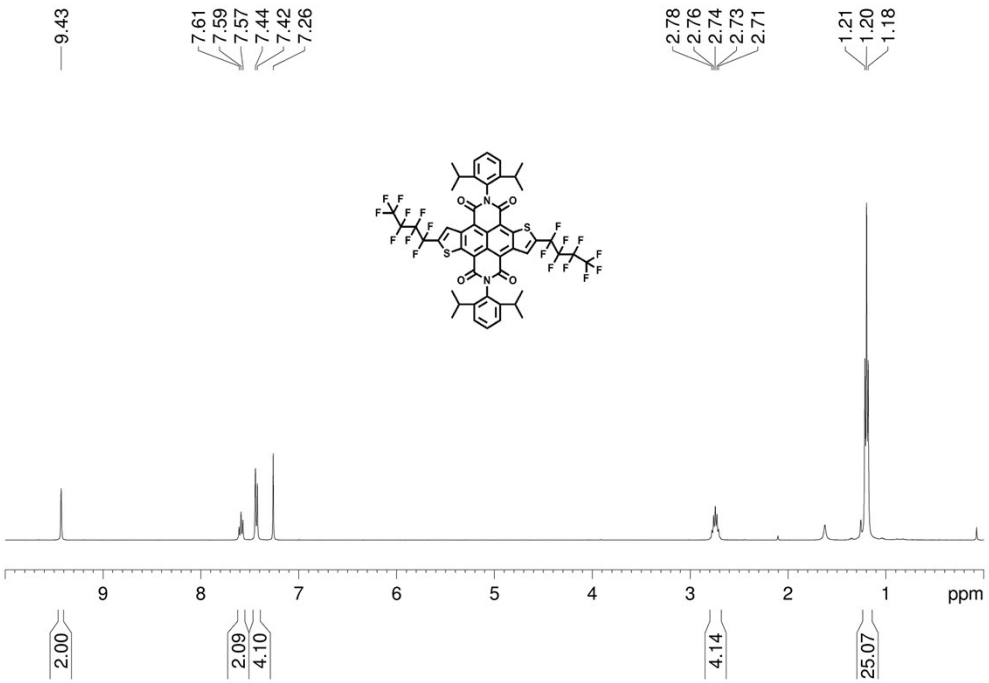

^{13}C NMR spectrum of **4** in $CDCl_3$

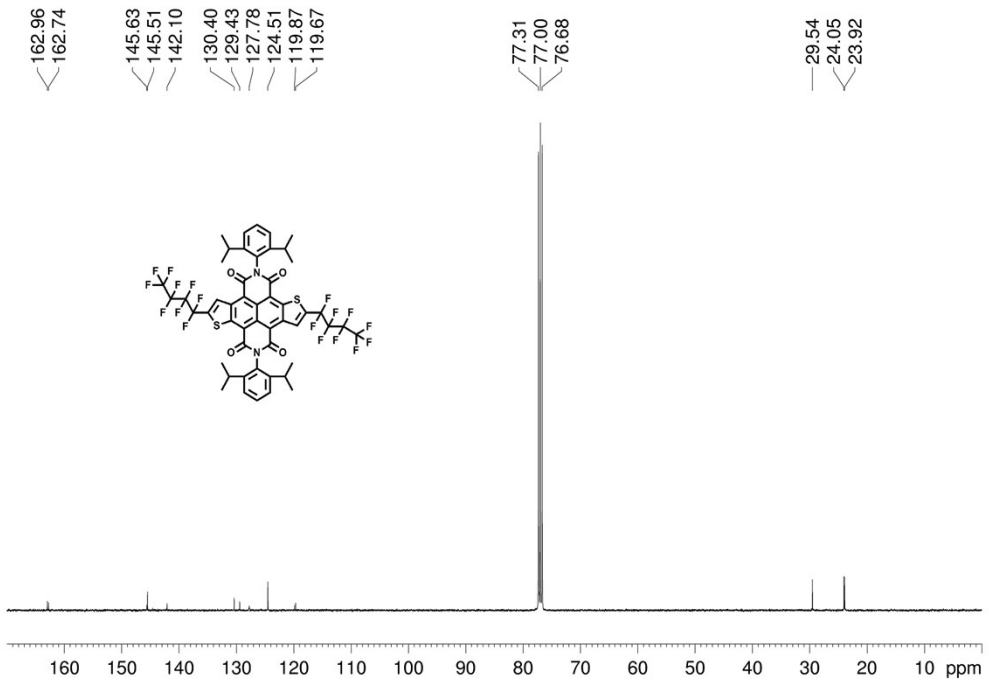

^{1}H NMR spectrum of **6** in $CDCl_3$

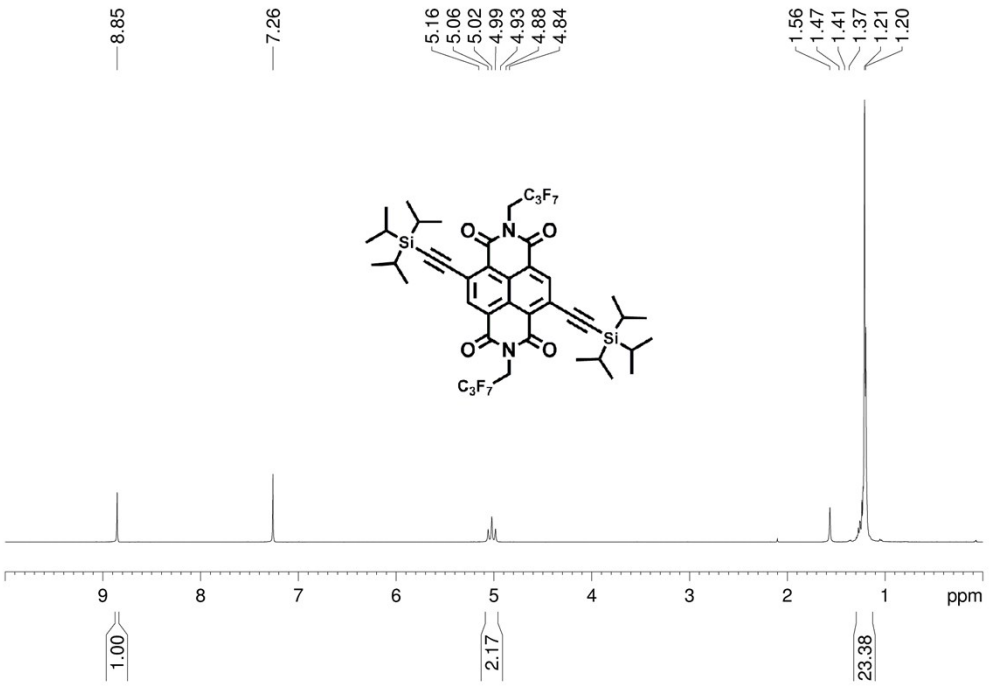

^{13}C NMR spectrum of **6** in $CDCl_3$

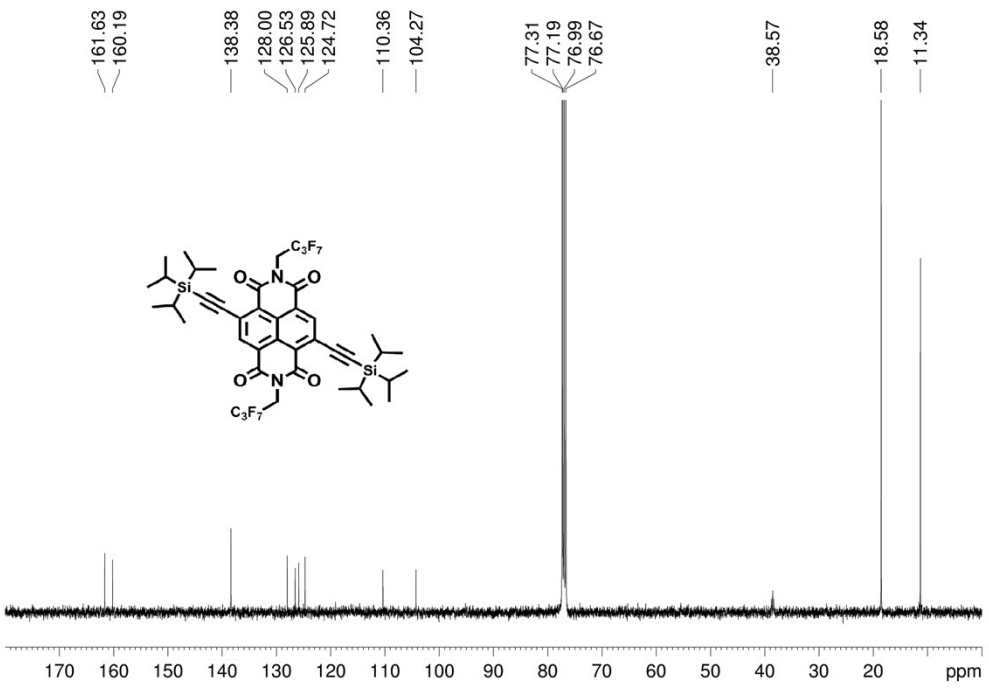

^{1}H NMR spectrum of **7** in $CDCl_3$

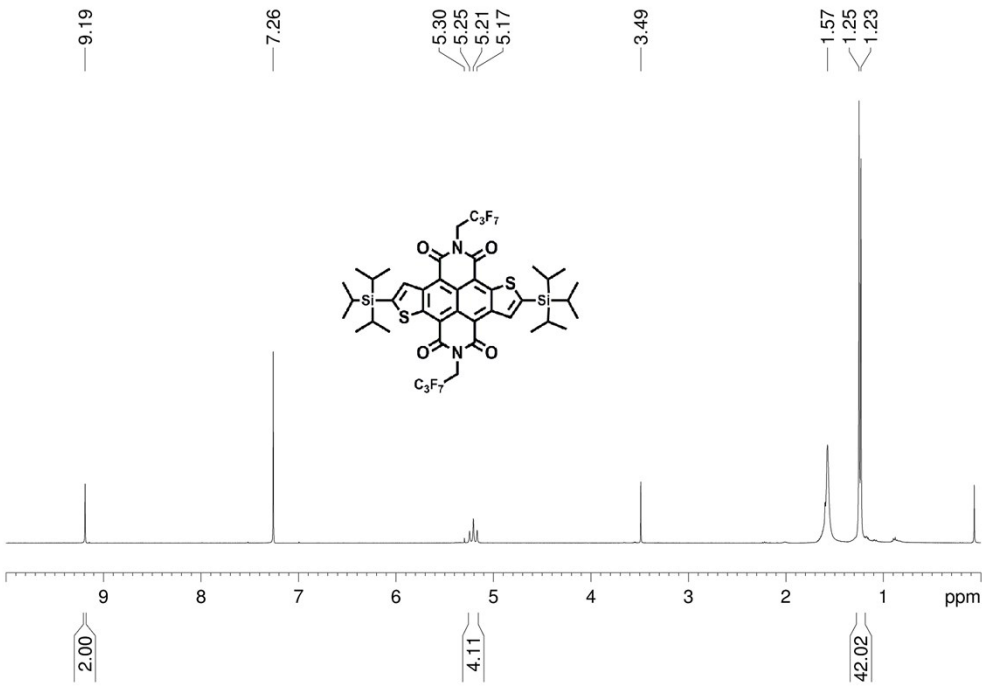

^{13}C NMR spectrum of **7** in $CDCl_3$

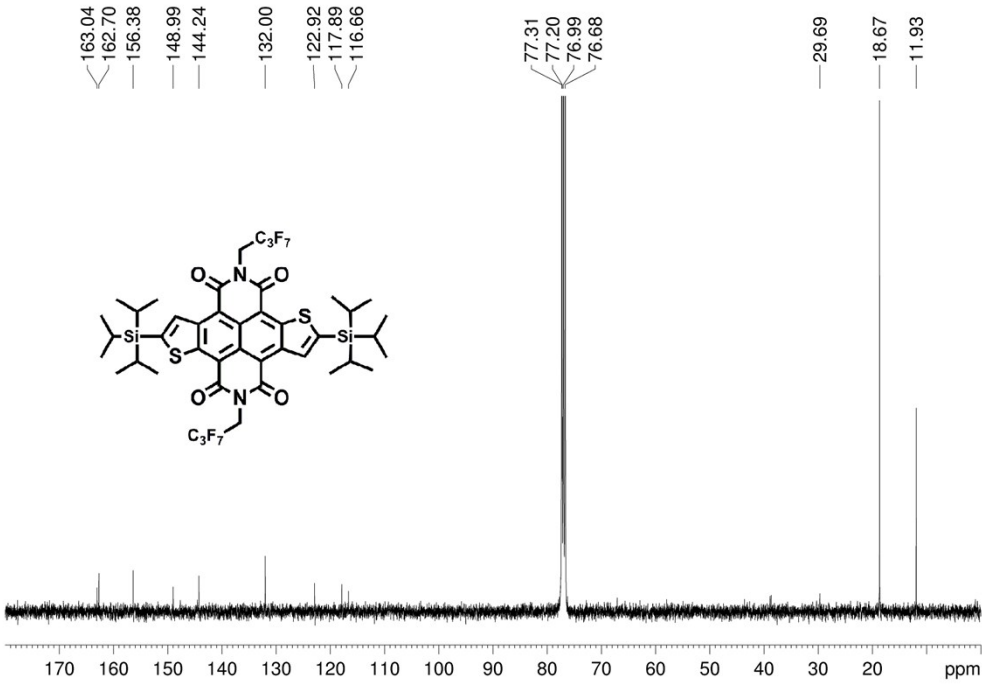

^{1}H NMR spectrum of **8** in $CDCl_2CDCl_2$